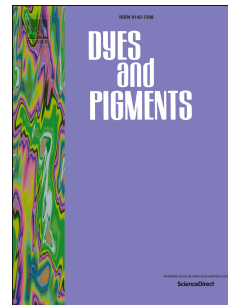


# Accepted Manuscript

Highly efficient chrysene emitters based on optimized side groups for deep blue emission

Seokwoo Kang, Hayoon Lee, Hoyocheol Jung, Minjin Jo, Mina Jung, Jongwook Park



PII: S0143-7208(18)30366-8

DOI: [10.1016/j.dyepig.2018.04.016](https://doi.org/10.1016/j.dyepig.2018.04.016)

Reference: DYPI 6677

To appear in: *Dyes and Pigments*

Received Date: 14 February 2018

Revised Date: 10 April 2018

Accepted Date: 10 April 2018

Please cite this article as: Kang S, Lee H, Jung H, Jo M, Jung M, Park J, Highly efficient chrysene emitters based on optimized side groups for deep blue emission, *Dyes and Pigments* (2018), doi: 10.1016/j.dyepig.2018.04.016.

This is a PDF file of an unedited manuscript that has been accepted for publication. As a service to our customers we are providing this early version of the manuscript. The manuscript will undergo copyediting, typesetting, and review of the resulting proof before it is published in its final form. Please note that during the production process errors may be discovered which could affect the content, and all legal disclaimers that apply to the journal pertain.

# Highly efficient chrysene emitters based on optimized side groups for deep blue emission

Seokwoo Kang<sup>a</sup>, Hayoon Lee<sup>a</sup>, Hyocheol Jung<sup>a</sup>, Minjin Jo<sup>b</sup>, Mina Jung<sup>b</sup>, Jongwook Park<sup>a\*</sup>

<sup>a</sup> Department of Chemical Engineering, Kyung Hee University, Gyeonggi, 17104, Korea

<sup>b</sup> Department of Chemistry/Display Research Center, The Catholic University of Korea

\*E-mail: jongpark@khu.ac.kr

## Abstract

Diphenylamine substituted with methyl groups was used as a side group to realize high efficiency chrysene deep blue emitters. Three chrysene derivatives substituted with side groups were successfully synthesized: tetra-*o*-tolylchrysene-6,12-diamine (*o*-DPAC), tetra-*m*-tolylchrysene-6,12-diamine (*m*-DPAC), and tetra-*p*-tolyl-chrysene-6,12-diamine (*p*-DPAC). The maximum PL (Photoluminescence) emission wavelengths of the three materials in solution and in a film were shortest for *o*-DPAC and longest for *p*-DPAC. The highly twisted structure of *o*-DPAC showed the narrowest FWHM (47 nm) in the deep blue region with a  $PL_{max}$  of 449 nm in the film state. The three synthesized materials showed excellent thermal stability with a high  $T_d$  over 370 °C. EML was applied to a non-doped OLED device considering the band gap of synthesized materials. Among the synthesized materials, the *m*-DPAC device achieved excellent EL performance of CIE  $x, y$  (0.14, 0.09), 4.89 cd/A, 3.60 lm/W, and an EQE of 6.18 %.

## 1. Introduction

Organic light emitting diodes (OLEDs) have been studied in various fields such as displays and biosensors due to their tunable optical and electronic properties. Organic light-emitting diodes (OLEDs) for displays were reported by the Tang group in 1987 and have been the subject of much research due to the applicability of full-color flat panel displays, next generation lighting, and flexible displays [1-6]. In OLEDs, electrons and holes are injected into the emitting layer, and emission is generated by the exciton formed inside. Thus, the characteristics of the emitting material are very important for determining the efficiency, wavelength, and lifetime of the OLED device. Therefore, it is essential to develop red, green, and blue emitting materials with pure color emission, high efficiency, and good thermal properties to realize full color OLED displays with high efficiency [7-12].

In particular, the Commission International de L'Eclairage (CIE) coordinates  $(x, y) = (0.14, 0.08)$

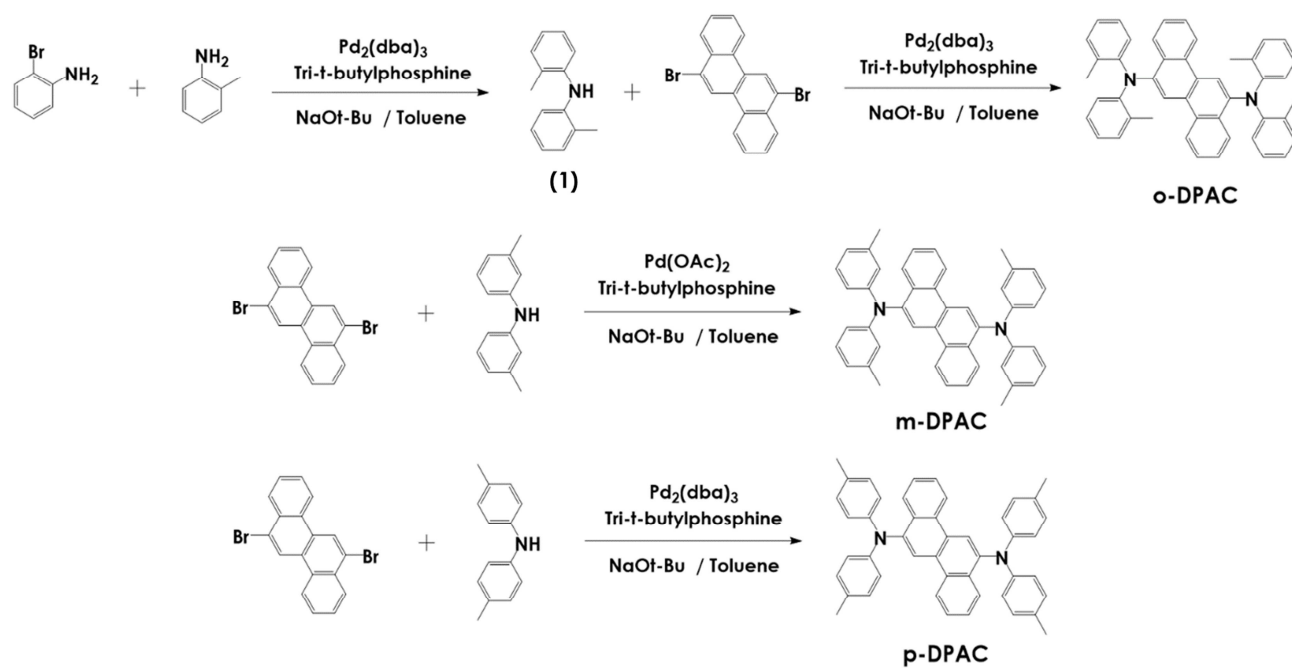
corresponding to deep blue were recently requested by the National Television System Committee (NTSC) standard. So, it is necessary to develop a stable deep blue emitting material with high efficiency. However, due to the wide band gap, which is the intrinsic property of blue light emitters, a large energy level difference exists with adjacent hole / electron transporting layers. Therefore, a high driving voltage is required for operation. During device operation, a higher voltage causes more joule heating, resulting in degradation of blue emitting materials, which in turn has a detrimental effect on lifetime and efficiency. Therefore, there is a continuing need for deep blue lighting materials with pure emission and high efficiency [13-17]. Although many studies on deep blue emitting materials have been reported, there are few papers on compounds that provide high efficiency [18-21]. Chrysene, anthracene, and pyrene show maximum absorbance wavelengths of 325 nm, 379 nm, and 338 nm, respectively. Chrysene especially absorbs light at shorter wavelength regions than other blue emitters. This implies that chrysene has an intrinsic short conjugation length, and its wide band gap is suitable for deep blue emission based on molecular design.

In our previous research, various deep blue emitter studies were carried out by introducing electron-donating groups and bulky side groups in chrysene. Among the developed compounds, DPA-C-DPA material (in which a diphenylamine group was introduced) showed an excimer peak in the film state, which resulted in poor efficiency and undesirable CIE (x, y) coordinates [22]. To solve this problem, we studied the effect of methyl group substituted diphenylamine groups at the ortho, meta, and para positions, effectively preventing excimer and deep blue emission. As previously reported, introducing a bulky group as a side group effectively prevents stacking between molecules, increasing color purity, efficiency, and device lifetime [16,17]. Therefore, we selected diphenylamine as the basic form of side groups and introduced methyl groups at the ortho, meta, and para sites to prevent self-quenching and reduce intermolecular interactions and aggregation through steric hindrance.

Thus, three new chrysene derivatives were synthesized: tetra-o-tolylchrysene-6,12-diamine (o-DPAC), tetra-m-tolylchrysene-6,12-diamine (m-DPAC), and tetra-p-tolylchrysene-6,12-diamine (p-DPAC). We used these materials as emitting layers (EMLs) of a non-doped device to determine the EL performance for these three derivatives.

## 2. Experimental

### 2.1. Synthesis



**Scheme 1.** Synthetic routes of the synthesized compounds.

**Compound (1) Di-*o*-tolyl-amine.** 1-Bromo-2-methylbenzene 1mL (8.39 mmol), *o*-toluidine 1.15mL,  $\text{Pd}_2(\text{dba})_3$  0.31g (0.336 mmol), sodium tert-butoxide 2.4g (25.2 mmol), and tri-*t*-butylphosphine 0.6mL (0.503 mmol) were added to 120 mL of anhydrous toluene in a 3-neck round bottom flask under a  $\text{N}_2$  atmosphere. After the reaction was finished, the mixture was extracted with ethyl acetate and DI water. The organic layer was dried with anhydrous  $\text{MgSO}_4$  and filtered. The solvent was evaporated. The crude product was purified by column chromatography on silica gel using THF: hexane = 1 : 20. (2.0g, Yield 27%)  $^1\text{H}$  NMR (300 MHz, DMSO):  $\delta$ (ppm) 8.25-8.22(m, 3H), 7.98-7.90(m, 8H), 7.55-7.41(m, 10H), 7.33-7.24(m, 8H), 7.19-7.11(m, 8H), 6.99(t, 2H).

**Tetra-*o*-tolylchrysene-6,12-diamine (o-DPAC).** Di-*o*-tolyl-amine 1.33g (6.77 mmol), 6,12-dibromochrysene 1.0g (2.60 mmol),  $\text{Pd}(\text{OAc})_2$  0.0468g (0.208 mmol), sodium tert-butoxide 1.5g (15.6 mmol), and tri-*t*-butylphosphine 0.37mL (0.313 mmol) were added to 100 mL of anhydrous toluene in a 3-neck round bottom flask under a  $\text{N}_2$  atmosphere. The mixture was refluxed at 110 °C for 10 h. After the reaction was finished, the mixture was extracted with chloroform and DI water. The organic layer was dried with anhydrous  $\text{MgSO}_4$  and filtered. The solvent was evaporated. The crude product was purified by column chromatography on silica gel using toluene: hexane = 1 : 10. (0.3g, Yield 19%)  $^1\text{H}$  NMR (300 MHz,

THF):  $\delta$ (ppm) 8.21-8.18(d, 1H), 8.08(s, 1H), 7.92-7.89(d, 1H), 7.47-7.41(t, 1H), 7.37-7.32(t, 1H), 7.23-7.19(t, 3H), 7.13-7.08(m, 1H), 6.99-6.88(m, 3H), 6.76-6.73(d, 1H), 2.48(s, 6H).  $^{13}\text{C}$ -NMR (75 MHz,  $\text{CDCl}_3$ ):  $\delta$ = 148.91, 148.13, 143.63, 134.17, 132.99, 132.21, 132.15, 131.98, 129.58, 127.19, 127.02, 126.73, 126.55, 126.00, 125.74, 125.22, 124.53, 124.28, 123.78, 117.72, 19.14; LRMS(EI, m/z):  $[\text{M}^+]$  calc'd. for  $\text{C}_{46}\text{H}_{38}\text{N}_2$ , 618.30; found, 618; Elemental analysis calc'd. (%) for  $\text{C}_{46}\text{H}_{38}\text{N}_2$ : C 89.28, H 6.19, N 4.53; found: C 87.28, H 6.26, N 4.17%.

**Tetra-*m*-tolylchrysene-6,12-diamine (m-DPAC).** Di-*o*-tolyl-amine 1.33g (6.77 mmol), 6,12-dibromochrysene 1.0g (2.60 mmol),  $\text{Pd}(\text{OAc})_2$  0.07g (0.312 mmol), sodium tert-butoxide 1.5g (15.6 mmol), and tri-tert-butylphosphine 0.37mL (0.313 mmol) were added to 100 mL of anhydrous toluene in a 3-neck round bottom flask under a  $\text{N}_2$  atmosphere. The mixture was refluxed at 110 °C for 10 h. After the reaction was finished, the mixture was extracted with chloroform and DI water. The organic layer was dried with anhydrous  $\text{MgSO}_4$  and filtered. The solvent was evaporated. The crude product was purified by column chromatography on silica gel using toluene: hexane = 1 : 3. (0.8g, Yield 50%)  $^1\text{H}$  NMR (300 MHz, THF):  $\delta$ (ppm) 8.63-8.60(m, 2H), 8.14-8.11(d, 1H), 7.58-7.52(t, 1H), 7.47-7.42(t, 1H), 7.09-7.04(t, 2H), 6.97(s, 2H), 6.92-6.89(d, 2H), 6.76-6.73(d, 2H), 2.18(s, 6H).  $^{13}\text{C}$ -NMR (75 MHz,  $\text{CDCl}_3$ ):  $\delta$ = 148.88, 143.07, 139.43, 132.27, 131.15, 129.35, 128.21, 127.35, 127.19, 125.53, 124.08, 122.99, 119.61, 21.80; LRMS(EI, m/z):  $[\text{M}^+]$  calc'd for  $\text{C}_{46}\text{H}_{38}\text{N}_2$ , 618.30; found, 618; Elemental analysis calc'd (%) for  $\text{C}_{46}\text{H}_{38}\text{N}_2$ : C 89.28, H 6.19, N 4.53; found: C 88.41, H 6.27, N 4.21%.

**Tetra-*p*-tolylchrysene-6,12-diamine (p-DPAC).** Di-*o*-tolyl-amine 1.33g (6.77 mmol), 6,12-dibromochrysene 1.0g (2.60 mmol),  $\text{Pd}(\text{OAc})_2$  0.07g (0.312 mmol), sodium tert-butoxide 1.5g (15.6 mmol) and tri-tert-butylphosphine 0.37mL (0.313 mmol) were added to 100 mL of anhydrous toluene in a 3-neck round bottom flask under a  $\text{N}_2$  atmosphere. The mixture was refluxed at 110 °C for 10 h. After the reaction was finished, the mixture was extracted with chloroform and DI water. The organic layer was dried with anhydrous  $\text{MgSO}_4$  and filtered. The solvent was evaporated. The crude product was purified by column chromatography on silica gel using toluene: hexane = 1 : 5. (0.44g, Yield 25%)  $^1\text{H}$  NMR (300 MHz, THF):  $\delta$ (ppm) 8.58-8.55(m, 2H), 8.11-8.08(d, 1H), 7.56-7.51(t, 1H), 7.44-7.39(t, 1H), 6.99(s, 8H), 2.25(s, 6H).  $^{13}\text{C}$ -NMR (75 MHz,  $\text{CDCl}_3$ ):  $\delta$ = 146.68, 143.21, 132.23, 131.47, 131.01, 130.16, 128.02, 127.21, 127.11, 125.51, 124.04, 122.50, 122.29, 20.97; LRMS(EI, m/z):  $[\text{M}^+]$  calc'd for  $\text{C}_{46}\text{H}_{38}\text{N}_2$ , 618.30; found, 618; Elemental analysis calc'd (%) for  $\text{C}_{46}\text{H}_{38}\text{N}_2$ : C 89.28, H 6.19, N 4.53; found: C 88.49, H 5.96, N 4.07%.

## 2.2. Materials, Measurements, and OLED Fabrication

Reactant di-*p*-tolylamine and 3,3'-dimethyldiphenylamine were purchased from Sigma-Aldrich and Alfa Aesar. Reagents and solvents were purchased as reagent grade and were used without further purification.

Analytical TLC was carried out on a Merck 60 F254 silica gel plate, and column chromatography was performed on Merck 60 silica gel (230-400 mesh). The  $^1\text{H-NMR}$  spectra were recorded on Bruker Advance 300 spectrometers. The FAB+-mass and EI+-spectra were recorded on a JMS-600W, JMS-700, 6890 Series, and Flash1112 or Flash2000. The optical UV-Vis absorption spectra were obtained using a Lambda 1050 UV/Vis/NIR spectrometer (Perkin Elmer). A Perkin-Elmer luminescence spectrometer LS55 (Xenon flash tube) was used to perform PL spectroscopy. The glass transition temperatures ( $T_g$ ) and melting temperatures ( $T_m$ ) of the compounds were obtained on a Differential Scanning Calorimetry (DSC) Discovery DSC25 (TA instruments) under a nitrogen atmosphere. Compounds were heated to 350 °C at rate of 5 °C/min and cooled at 5 °C/min. Degradation temperatures ( $T_d$ ) values of the compounds were measured with Thermal Gravimetric Analysis (TGA) using a TGA4000 (Perkin Elmer). Samples were heated to 700 °C at a rate of 10 °C/min. The HOMO energy levels were determined with ultraviolet photoelectron spectroscopy (Riken Keiki AC-2). The LUMO energy levels were derived from the HOMO energy levels and the band gaps. For the EL devices, all organic layers were deposited under  $10^{-6}$  torr, with a rate of deposition of 1 Å/s to give a deposition area of 4 mm<sup>2</sup>. The LiF and aluminum layers were continuously deposited under the same vacuum condition. The current-voltage-luminance (I-V-L) characteristics of the fabricated EL devices were obtained with a Keithley 2400 electrometer. Light intensities were obtained with a Minolta CS-1000A. The device was stored in a glovebox for stability against moisture and air.

### 3. Results and Discussion

#### Molecular design, optical properties, and thermal properties

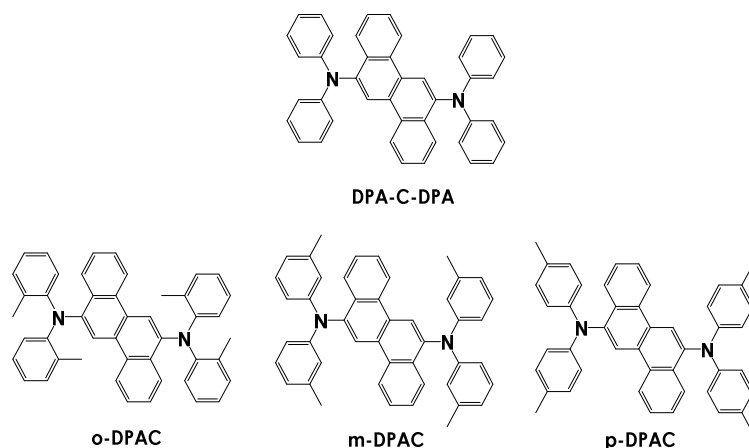


**Fig. 1.** Chemical structures of the chrysene derivatives.

Fig. 1 and Scheme 1 show the chemical structures and synthetic method used to make the materials. Chrysene was selected as the core chromophore. Diphenylamine substituted with methyl groups was used as a side group, and the substitution position of the methyl group was changed to the ortho, meta, and para positions based on the amine group. To compare the optical and electrical properties with the three newly synthesized materials, a previously reported diphenylamine-substituted chrysene derivative (DPA-C-DPA) without the methyl group was selected as the reference material [22]. Synthesis was performed using a conventional Suzuki-Miyaura cross-coupling reaction. All compounds were purified by recrystallization and column chromatography. The synthesized compounds were characterized using nuclear magnetic resonance (NMR) spectroscopy, mass spectroscopy, and elemental analysis.

Fig. 2 and 3 show UV-visible (UV-VIS) absorption and photoluminescence (PL) spectra of the synthesized compounds in a toluene solution and as a vacuum deposited film, respectively. Table 1 summarizes the optical properties, thermal properties, and energy levels of these compounds

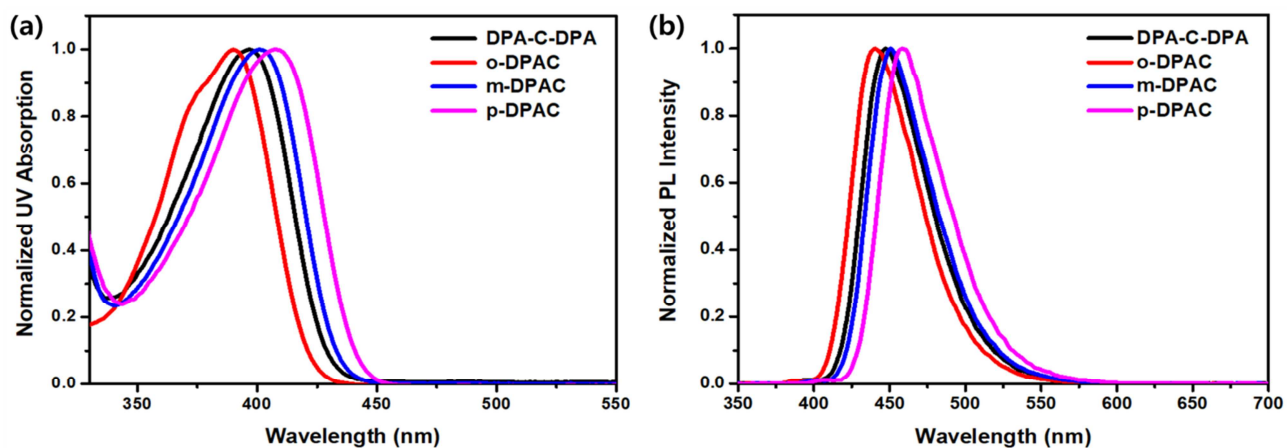


Fig. 2. (a) UV-VIS absorption and (b) PL spectra of  $1 \times 10^{-5}$  M toluene solution for the synthesized materials.

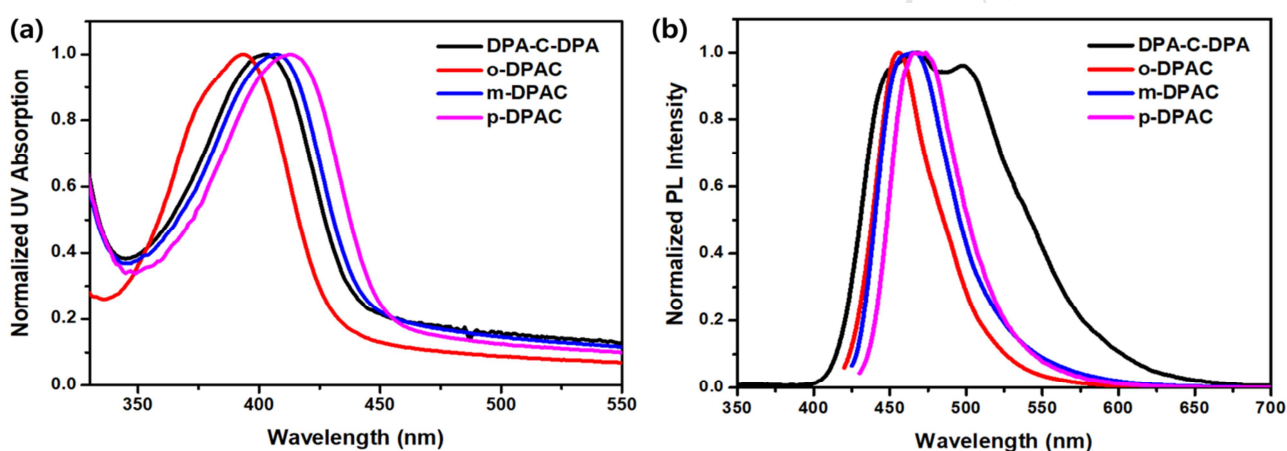


Fig. 3. (a) UV-VIS absorption and (b) PL spectra of the vacuum-deposited film for the synthesized materials.

Table 1. Optical, thermal, and electrical properties of the synthesized compounds.

	Solution <sup>a</sup>			Film on glass <sup>b</sup>			$\Phi_f^d$	$T_g$ (°C)	$T_m$ (°C)	$T_d$ (°C)	HOMO <sup>e</sup> (eV)	LUMO (eV)	Band gap (eV)
	UV <sub>max</sub> (nm)	PL <sub>max</sub> (nm)	FWHM <sup>c</sup> (nm)	UV <sub>max</sub> (nm)	PL <sub>max</sub> (nm)	FWHM (nm)							
DPA-C-DPA	395	447	50	402	464, 501	80	32	198	321	361	-5.49	-2.67	2.82
o-DPAC	390	440	50	393	449	47	67	-	-	379	-5.47	-2.55	2.92
m-DPAC	401	450	50	407	454	55	92	248	308	370	-5.4	-2.57	2.83
p-DPAC	408	459	51	413	462	53	90	263	314	415	-5.37	-2.59	2.78

<sup>a</sup> Toluene solution ( $1.00 \times 10^{-5}$  M). <sup>b</sup> Film thickness is 50 nm on the glass. <sup>c</sup> Full width at half maximum of PL. <sup>d</sup> Absolute PLQY of 1 wt% dispersed film in PMMA. <sup>e</sup> Ultraviolet photoelectron spectroscopy (Riken-Keiki, AC-2).

The maximum UV-VIS absorption wavelength of the three synthesized materials was a 5 nm blue shift for o-DPAC and a 6 nm red for m-DPAC compared to the reference material DPA-C-DPA in the solution state. In the case of p-DPAC, the maximum absorption wavelength was 408 nm, or a 13 nm red shift. The maximum PL emission wavelength of the solution state was 447 nm for the reference DPA-C-DPA, and the maximum PL emission of o-DPAC showed a blue shifted wavelength of 440 nm, which is the shortest among the three synthesized materials. This is because the methyl group in the ortho position has a highly twisted structure due to repulsion between the core and the side group, which resulted in a larger band gap. In m-DPAC, the electron-donating effect and the twisted angle were relatively weak due to the methyl group at the meta position, and the maximum PL wavelength was 450 nm. In p-DPAC, the methyl group of the para position does not cause steric hindrance with the core group, and it even provides an electron-donating effect for the core moiety. So, the twisted structure is reduced, and the maximum PL wavelength value is shown at 459 nm, which is the longest.

In the solution state, FWHM values showed similar values (50 nm) for all four materials. In the film state of DPA-C-DPA, an excimer peak was formed at 501 nm in addition to 464 nm, while excimer peaks were not observed in all three new diphenylamine derivatives substituted with methyl groups. This means that the introduction of methyl groups effectively prevented intermolecular packing. In the o-DPAC, methyl substitution at the ortho position effectively prevented packing in the film state and showed a maximum emission wavelength at 449 nm. In the m-DPAC, the electron-donating effect was weak due to the introduction of a methyl group at the meta position, and the steric hindrance effect partially acts to prevent the excimer, resulting in a maximum emission wavelength of 454 nm. In p-DPAC, the intermolecular packing was effectively prevented due to introduction of the methyl group, and the maximum emission wavelength of 462 nm was observed due to the electron-donating effect at the para position.

In the solution state, the DPA-C-DPA material had a FWHM of 50 nm; that in the film state was large at

80 nm. On the other hand, the three synthesized materials showed an FWHM value of 47-55 nm, which is relatively narrow in both in the solution and film state. Especially, in the case of o-DPAC compound, film and solution states showed similar FWHM values of 47 nm and 50 nm. Film state has larger value of FWHM compared to solution state in general, but o-DPAC did not have this result tendency. It may be due to the prevention of molecular packing which comes from the large dihedral angle of o-DPAC compound in film state. The maximum PL wavelength value of the three compounds in the film state showed a tendency to red shift 3-9 nm relative to that in the solution.

Optimized structures and dihedral angles of the three materials were calculated using Gaussian density functional theory (DFT) as shown in Fig. 4. The dihedral angle (a-b-c-d,  $\alpha$  position) of the core and side of DPA-C-DPA was 47.72°. o-DPAC had the largest angle of 65.83°, and the steric hindrance between the core and the side group greatly contributed to the degree of twisting. As a result, the maximum PL emission wavelength was 449 nm, which is the blue-shifted region in the film state. In addition, intermolecular packing can be effectively prevented in the film state, and the FWHM value remained narrow [23,24]. Dihedral angles of m-DPAC and p-DPAC were  $\alpha = 53.84$  and  $53.08$ °, respectively. All of synthesized materials including methyl group had increased dihedral angle compared to DPA-C-DPA. It caused to the twisted chemical structure and preventing intermolecular packing.

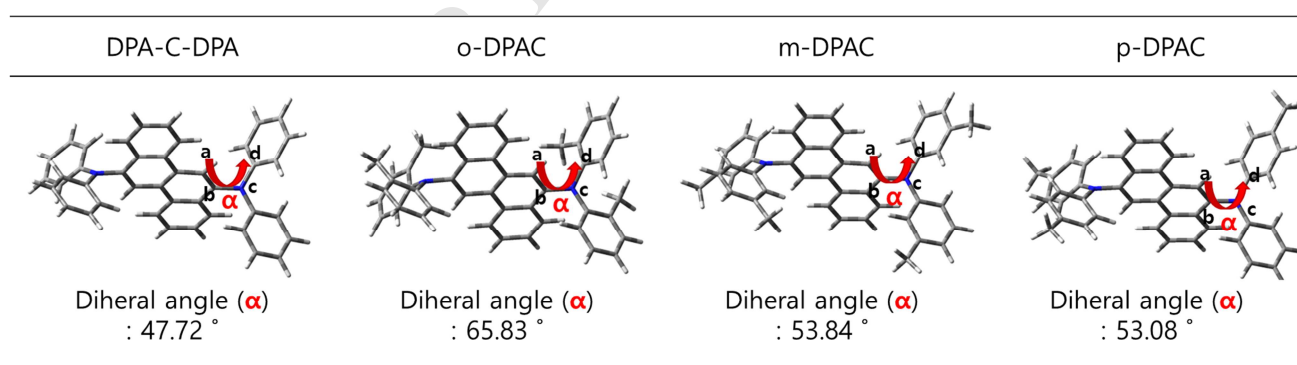


**Fig. 4.** Optimized structures and dihedral angles of chrysene derivatives: DPA-C-DPA, o-DPAC, m-DPAC, and p-DPAC (calculated at the B3LYP/6-31G(d)).

Density functional theory (DFT) calculations were carried out to confirm the property change when diphenylamine groups substituted with methyl groups were introduced into the chrysene core. The

electron density distribution of the highest occupied molecular orbital (HOMO) of the four chrysenes derivatives is

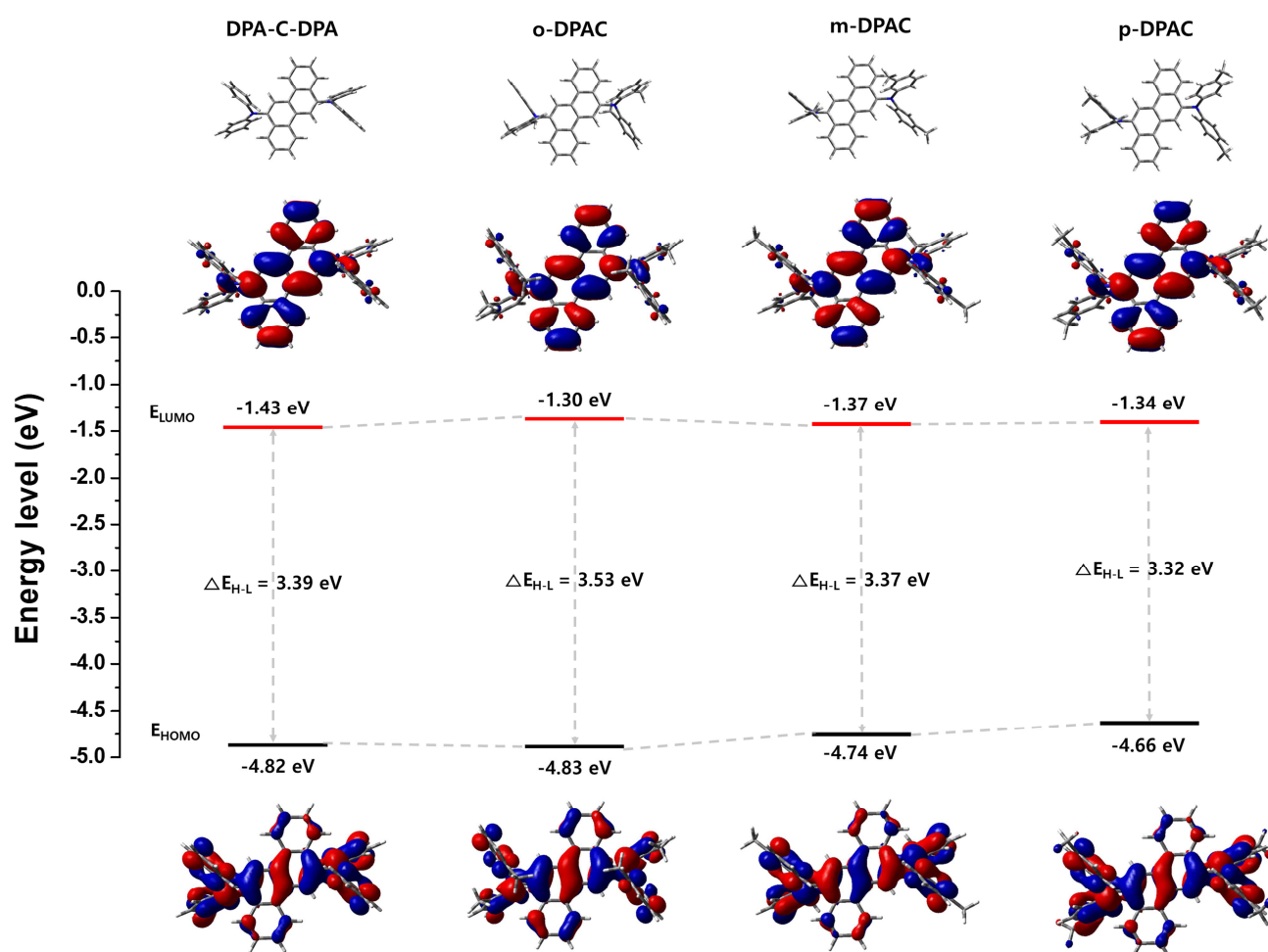


**Fig. 5.** Pictorial presentation of the frontier orbitals and a plot of HOMO and LUMO energy levels for DPA-C-DPA, o-DPAC, m-DPAC, and p-DPAC (calculated at the B3LYP/6-31G(d)).

widely distributed throughout the chrysenes and side groups. On the other hand, the electron density distribution of the lowest unoccupied molecular orbital (LUMO) is localized in the chrysenes core because of the electron-donating effect of the side group. The HOMO and LUMO were -5.49 to -5.37 eV and -2.67 to -2.55 eV, respectively. The calculated band gap ( $\Delta E_{\text{H-L}}$ ) follows the order of o-DPAC (3.53 eV) > m-DPAC

(3.37 eV) > p-DPAC (3.32 eV). The measured band gaps were 2.92 eV, 2.83 eV, and 2.78 eV, which followed the same trend as that of calculated values (Table 1, Fig. 5).

Absolute photoluminescence quantum yields (PLQYs) were measured by fabricating 1 wt% doped films on

poly(methyl methacrylate) (PMMA). PLQYs values of DPA-C-DPA, o-DPAC, m-DPAC, and p-DPAC were 32 %, 67 %, 92 %, and 90 %, respectively (Table 1). m-DPAC showed a value of 92 %, the highest among the four compounds. Since the PLQY value of the emitter is an important factor for determining the EL efficiency of the OLED device, m-DPAC and p-DPAC are expected to exhibit excellent EL efficiency when used in OLED devices as a blue light emitting material.

The glass transition temperature ( $T_g$ ), melting temperature ( $T_m$ ), and decomposition temperature ( $T_d$ ) of the synthesized materials were measured by DSC and TGA, respectively as shown in Table 1 and Fig. 6.  $T_g$  value of more than 100 °C is required for commercialization of OLED displays. Two compounds of m-DPAC, and p-DPAC showed  $T_g$  values of 248 °C and 263 °C which is higher than 198 °C of DPA-C-DPA. Two compounds also had  $T_m$  values of 308 °C and 314 °C. o-DPAC did not show  $T_g$  and  $T_m$  values. The  $T_d$  values of o-DPAC, m-DPAC, and p-DPAC are 379, 370, and 415 °C, respectively, while the  $T_d$  value is 361 °C for DPA-C-DPA. It is because the introduction of the methyl group leads to an increase in molecular weight, thereby improving the thermal stability. This high thermal property can provide stable device morphology under the heat generated during OLED device operation [25].

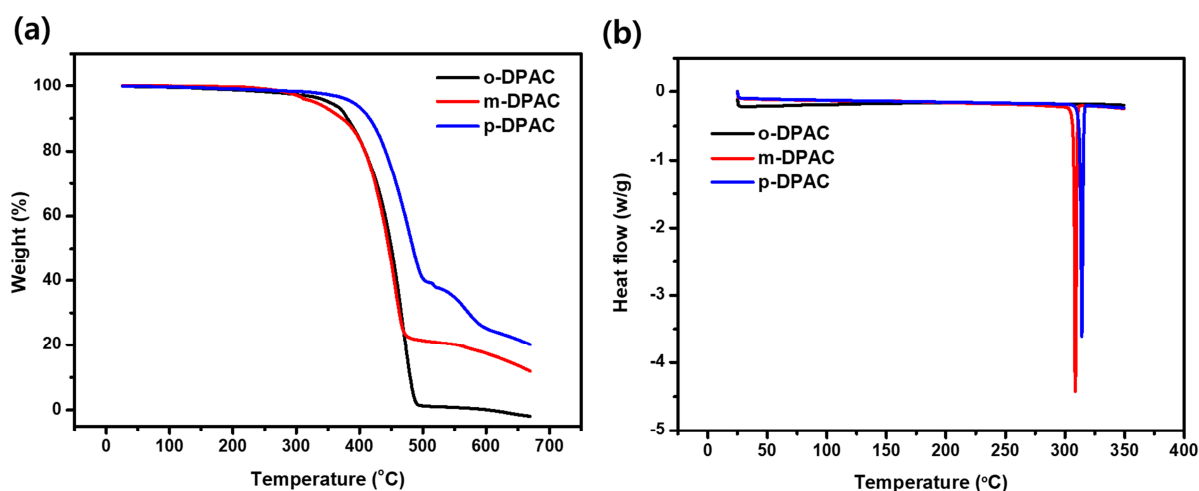


Fig. 6. Thermal properties of the chrysene derivatives: (a) TGA and (b) DSC

### Electroluminescence properties

EL performance was observed using OLED devices to confirm the side group effect with methyl group substitution. The synthesized materials were used as the non-doped emitting layer. Devices were

fabricated with the configuration of ITO / N,N'-bis(naphthalene-1-yl)-N,N'-bis(phenyl)benzidine (NPB), 40 nm / synthesized emitting materials, 30 nm / 1,3,5-tri(1-phenyl-1H-benzo[d]imidazole-2-yl)phenyl (TPBi), 30 nm / LiF, 1 nm / Al, 200 nm. NPB was used as the hole-injection and transporting layer. TPBi was used as the electron-transporting and hole-blocking layer.

The performances of the OLED devices are shown in Fig. 7 and Fig. 8, and the results are summarized in Table 2. Fig. 7-(a) shows current density and luminance as a function of the applied voltage. Normal diode characteristic curves were observed. Fig. 7-(b), (c), and (d) show three efficiencies based on the current

**Table 2.** EL performances of synthesized materials.

Compounds	$V_{on}$ (V) <sup>a</sup>	LE (cd/A) <sup>b</sup>	PE (lm/W) <sup>c</sup>	EQE (%) <sup>d</sup>	CIE (x, y) <sup>e</sup>	EL <sub>max</sub> (nm)	PL <sub>max</sub> (nm)
DPA-C-DPA	5.47	2.16	1.38	1.80	0.17, 0.15	454, 548	464, 501
o-DPAC	3.49	2.67	2.46	4.01	0.15, 0.08	446	449
m-DPAC	3.84	4.89	3.60	6.18	0.14, 0.09	450	454
p-DPAC	3.42	4.39	4.07	4.09	0.14, 0.14	460	462

<sup>a</sup> Operating voltage at 10mA/cm<sup>2</sup>. <sup>b</sup> Luminance efficiency. <sup>c</sup> Power efficiency. <sup>d</sup> External quantum efficiency. <sup>e</sup> Commission International de l'Eclairage.

density in the range of 0 to 50 mA/cm<sup>2</sup>. Three graphs show stable efficiencies at high current density and low current density. As shown in Table 2, the EL<sub>max</sub> values of the three compounds are similar to the PL<sub>max</sub> values. This means that EL light emitted from the device is consistent with the emitter emission. o-DPAC, m-DPAC, and p-DPAC have luminance efficiency values of 2.67, 4.89, and 4.39 cd/A, respectively, while that of the reference material DPA-C-DPA is 2.16 cd/A. All three materials had efficiencies that were 23-126 % higher than that of DPA-C-DPA without methyl groups. m-DPAC showed the best luminance efficiency among the four materials. This result is due to the electron-donating effect of the methyl group. The CIE (x, y) value shows that the three synthesized materials had reduced y-coordinate values compared to that of DPA-C-DPA and thus had excellent blue luminescence properties. This is consistent with the

tendency of the  $EL_{max}$  values. EQE values can be determined based on the luminance efficiency and CIE value.

The EQE value of the DPA-C-DPA was 1.8 %, but those of the three synthesized materials were 4.01-6.18 %, which is an increase of 122-243%. Especially, m-DPAC exhibited EQE value of 6.18 % which is over 5 %. EQE value is determined by four factors which are the light out-coupling factor, the ratio of singlet or triplet exciton, the photoluminescence quantum yield, and the carrier balance. Based on our previous study, it may be explained by the increased light out-coupling factor and the increased ratio of singlet exciton. Light out-coupling factor can be enhanced by horizontal orientation of emitter film during thermal deposition and the ratio of singlet exciton can be increased by triplet-triplet annihilation during device operation. Further studies are underway [26,27]. The operating voltage at a current density of 10 mA/cm<sup>2</sup> was also found to be 3.42-3.84 V lower than that of the reference material, which resulted in better power efficiency than for DPA-C-DPA.

Fig. 8 shows (a) EL spectra and (b) CIE (x, y) values for the synthesized materials, and (c) band diagram of materials using OLED device. Smaller x and y coordinate values indicate better performance for blue colors. In particular, the y coordinate value must be 0.15 or less for a mobile phone and 0.08 or less for a TV. For the reference material, x and y coordinate values are shown at the highest position, while all the synthesized materials show better x and y coordinate values. In particular, o-DPAC showed an NTSC y coordinate value of 0.08, and m-DPAC, which had the highest luminance efficiency, showed 0.09, which is very close to the NTSC y coordinate value.

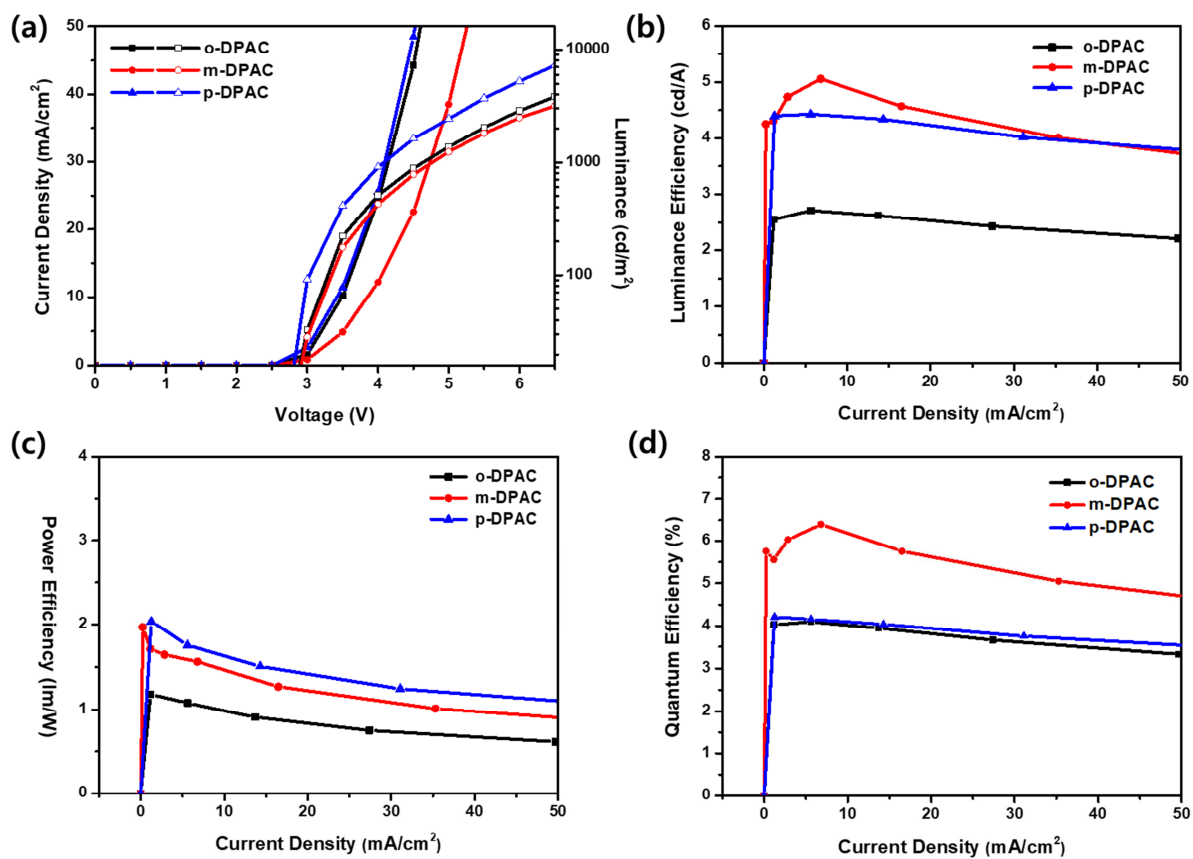


**Fig. 7.** EL characteristics of devices using o-DPAC, m-DPAC, and p-DPAC as EMLs: (a) I-V-L curve, (b) luminance efficiency versus current density, (c) power efficiency versus current density, and (d) external quantum efficiency versus current density.

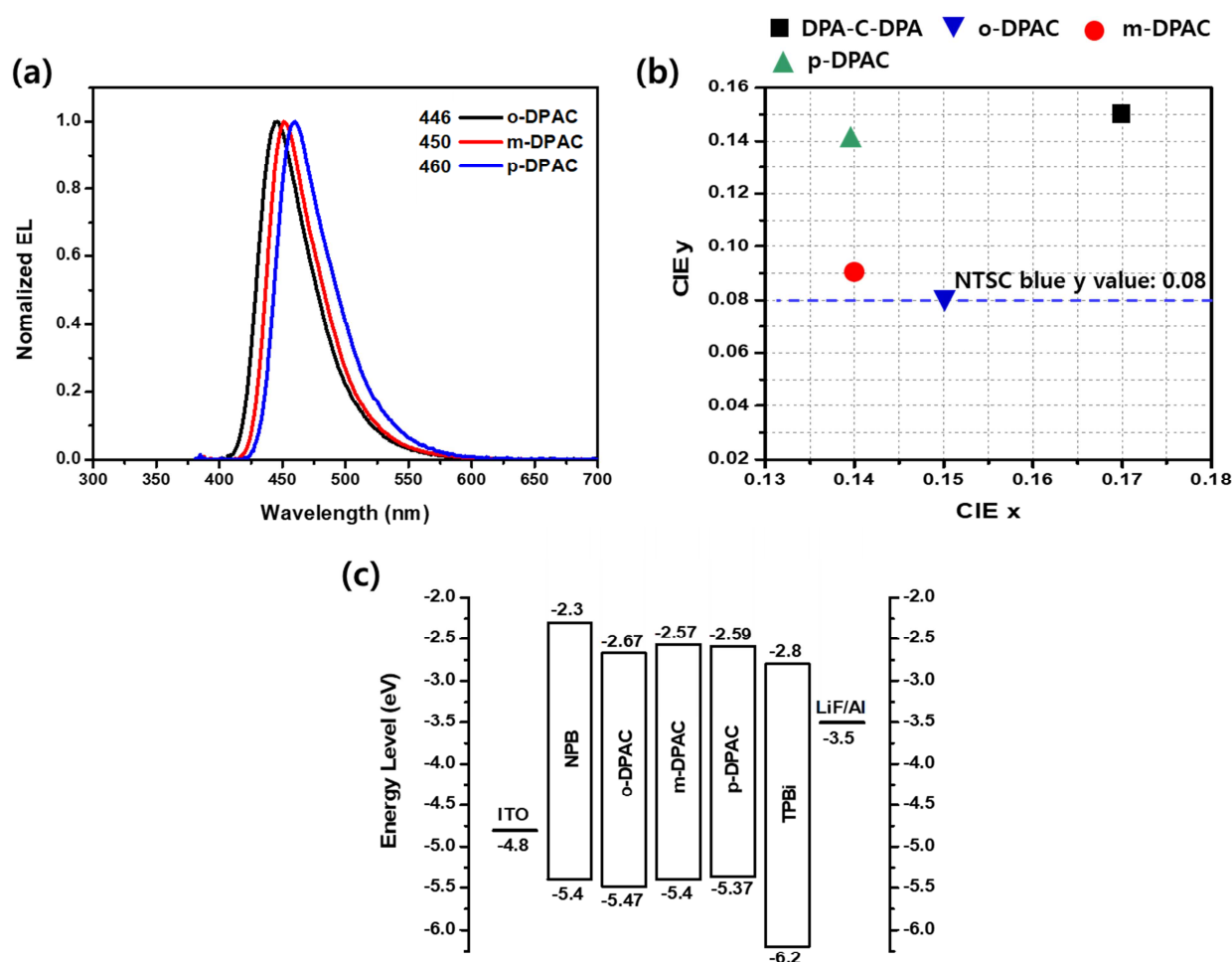


**Fig. 8.** (a) EL spectra of devices and (b) CIE x, y values of the synthesized compounds, and (c) band diagram of materials using OLED device.

#### 4. Conclusion

o-DPAC, m-DPAC, and p-DPAC were successfully synthesized by replacing the methyl group substituted in the ortho, meta, and para positions of diphenylamine with a chrysene core. The optical properties of the synthesized materials show the same tendency to red shift according to the ortho, meta, and para substitution positions of the methyl group in both solution and film states. o-DPAC showed the highest dihedral angle ( $65.83^\circ$ ) due to the introduction of the methyl group at the ortho position, indicating a highly twisted structure. Among the synthesized materials, the maximum emission wavelength was observed for o-DPAC at 449 nm, which is the most blue-shifted region in the film state. The synthesized materials were applied to a non-doped OLED device as an EML. o-DPAC, which had the widest band gap, showed deep blue emission of CIE x, y (0.14, 0.08) and an EQE of 4.01 %. m-DPAC exhibited the highest luminance value of 4.89 cd/A among the four materials and an EQE of 6.18 %, which was about 54 % higher than those of the other two materials. Optimization of side groups would be very helpful for the development of high EL efficiency and high color purity deep blue emitting material.

## Acknowledgements

This research was supported by National R&D Program through the National Research Foundation of Korea (NRF) funded by the Ministry of Science & ICT (No. 2017M3A7B4041699). This research was supported by Basic Science Research Program through the National Research Foundation of Korea(NRF) funded by the Ministry of Education (No. 2017R1D1A1A09082138)

## References

- [1] Tang CW, Vanslyke SA. Organic electroluminescent diodes. *Appl Phys Lett* 1987;51:913.
- [2] Kim JS, Heo J, Kang P, Kim JH, Jung SO, Kwon SK. Synthesis and characterization of organic light-emitting copolymers containing naphthalene. *Macromol Res* 2009;17:91.
- [3] Park HT, Shin DC, Shin SC, Kim JH, Kwon SK, Kim YH. Synthesis and characterization of blue light emitting polymers based on arylene vinylene. *Macromol Res* 2011;19:965.
- [4] (a) Gelinas S, Rao A, Kumar A, Smith SL, Chin AW, Clark J, et al. Ultrafast long-range charge separation in organic semiconductor photovoltaic diodes. *Science* 2014;343:512. (b) Forrest SR, Baldo MA, Thompson ME. High-efficiency fluorescent organic light-emitting devices using a phosphorescent sensitizer. *Nature* 2000;403:750.
- [5] Kim SK, Park YI, Kang IN, Lee JH, Park J. New deep-blue emitting materials based on fully substituted ethylene derivatives. *J Mater Chem* 2007;17:4670.
- [6] Kim SH, Kim BJ, Lee JH, Shin HG, Park YI, Park JW. Design of fluorescent blue light-emitting materials based on analyses of chemical structures and their effects. *Materials Science and Engineering R* 2016;99:1.
- [7] Lee S, Kim KH, Limbach D, Park YS, Kim JJ. Low roll-off and high efficiency orange organic light emitting diodes with controlled co-doping of green and red phosphorescent dopants in an exciplex forming co-host. *Adv Funct Mater* 2013;23:4105.
- [8] Kuei CY, Tsai WL, Tong B, Jiao M, Lee WK, Chi Y, et al. Bis-tridentate Ir(III) complexes with nearly unitary RGB phosphorescence and organic light emitting diodes with external quantum efficiency exceeding 31 %. *Adv Mater* 2016;28:2795.
- [9] Giridhar T, Han TH, Cho W, Saravanan C, Lee TW, Jin SH. An easy route to red emitting homoleptic Ir<sup>III</sup> complex for highly efficient solution-processed phosphorescent organic light-emitting diodes. *Chem Eur J* 2014;20:8260.
- [10] Uoyama H, Goushi K, Shizu K, Nomura H, Adachi C. Highly efficient organic light-emitting diodes

from delayed fluorescence. *Nature* 2012;492:234.

[11] Fleetham T, Ecton J, Li G, Li J. Improved out-coupling efficiency from a green microcavity OLED with a narrow band emission source. *Org Electron* 2016;37:141.

[12] Komatsu R, Sasabe H, Seino Y, Nakao K, Kido J. Light-blue thermally activated delayed fluorescent emitters realizing a high external quantum efficiency of 25% and unprecedented low drive voltages in OLEDs. *J Mater Chem C* 2016;4:2274.

[13] Zhang D, Cai M, Bin Z, Zhang Y, Zhang D, Duan L. Highly efficient blue thermally activated delayed fluorescent OLEDs with record-low driving voltages utilizing high triplet energy hosts with small singlet-triplet splittings. *Chem Sci* 2016;7:3355.

[14] Kim SK, Yang B, Ma Y, Lee JH, Park J. Exceedingly efficient deep-blue electroluminescence from new anthracenes obtained using rational molecular design. *J Mater Chem* 2008;18:3376.

[15] Kim SK, Yang B, Park YI, Ma Y, Lee JY, Kim HJ, et al. Synthesis and electroluminescent properties of highly efficient anthracene derivatives with bulky side groups. *Org Electron* 2009;10:822.

[16] Kim B, Park Y, Lee J, Yokoyama D, Lee JH, Kido J, et al. Synthesis and electroluminescence properties of highly efficient blue fluorescence emitters using dual core chromophores. *J Mater Chem C* 2013;1:432.

[17] Lee H, Kim B, Kim S, Kim J, Lee J, Shin H, et al. Synthesis and electroluminescence properties of highly efficient dual core chromophores with side groups for blue emission. *J Mater Chem C* 2014;2:4737.

[18] Chenglong L, Jinbei W, Jianxiong H, Zhiqiang L, Xiaoxian S, Zuolun Z, Jingying Z, Yue W. Efficient deep-blue OLEDs based on phenanthro[9,10-d]imidazole-containing emitters with AIE and bipolar transporting properties. *J Mater Chem C* 2016;4:10120.

[19] Xuejun Z, Zhongbin W, Yuxuan L, Yujun X, Qian P, Qianqian L, Dongge M, Zhen L. Benzene-cored AIEgens for deep-blue OLEDs: high performance without hole-transporting layers, and unexpected excellent host for orange emission as a side-effect. *Chem Sci* 2016;7:4355.

[20] Wei S, Nonglin Z, Yin X, Shirong W, Xianggao L. A Novel Spiro[acridine-9,9'-fluorene] Derivatives Containing Phenanthroimidazole Moiety for Deep-Blue OLED Application. *Chem Asian J* 2017; accepted

[21] Ramiro C, Min C, Brian T, David LW, Rajiv K, Ayuna T, Aime'e LT, Ruth S, Joseph S, Malika J. Benzobisoxazole cruciforms: a tunable, crossconjugated platform for the generation of deep blue OLED materials. *J Mater Chem C* 2016;4:3765.

[22] Shin H, Jung H, Kim B, Lee J, Moon J, Kim J, Park J. Highly efficient emitters of ultra-deep-blue light made from chrysene chromophores. *J Mater Chem C* 2016;4:3833.

[23] Krzysztof D, Tai-Hsiang H, Jiann TL, Yu-Tai T, Chang-Hao C. Blue-Emitting Anthracenes with End-

Capping Diarylamines. *Chem Mater* 2002;14:3860.

[24] Ping-I S, Chu-Ying C, Chen-Han C, Eric Wei-GD, Ching-Fong S. Highly Efficient Non-Doped Blue-Light-Emitting Diodes Based on an Anthracene Derivative End-Capped with Tetraphenylethylene Groups. *Adv Funct Mater* 2007;17:3141.

[25] Park YI, Kim B, Lee C, Hyun A, Jang S, Lee JH, Gal YS, Kim TH, Kim KS, Park J. Highly Efficient New Hole Injection Materials for OLEDs Based on Dimeric Phenothiazine and Phenoxazine Derivatives. *J Phys Chem C* 2011;115:4843.

[26] B Kim, Y Park, J Lee, D Yokoyama, JH Lee, J Kido, and J Park. Synthesis and electroluminescence properties of highly efficient blue fluorescence emitters using dual core chromophores. *J Mater Chem C* 2013;1:432.

[27] D Yokoyama, Y Park, B Kim, S Kim, YJ Pu, J Kido, and J Park. Dual efficiency enhancement by delayed fluorescence and dipole orientation in high-efficiency fluorescent organic light-emitting diodes. *Appl Phys Lett* 2011;99:123303.

- Diphenylamine substituted with methyl groups was used as a side group to realize high efficiency chrysene deep blue emitters.
- The synthesized emitters showed excellent thermal stability with a high  $T_d$  over 370 °C.
- m-DPAC compound among the synthesized materials achieved excellent blue EL performance of CIE x, y (0.14, 0.09), 4.89 cd/A, and an EQE of 6.18 %.